

Constraining the Radii of Neutron Stars with Terrestrial Nuclear Laboratory Data

Bao-An Li

*Department of Physics, Texas A&M University-Commerce, P.O. Box 3011,
Commerce, TX 75429-3011, USA
and Department of Chemistry and Physics, P.O. Box 419, Arkansas State
University, State University, Arkansas 72467-0419, USA*

Andrew W. Steiner

*Theoretical Division, Los Alamos National Laboratory, Los Alamos, NM 87545,
USA*

Abstract

Neutron star radii are primarily determined by the pressure of isospin asymmetric matter which is proportional to the slope of the nuclear symmetry energy. Available terrestrial laboratory data on the isospin diffusion in heavy-ion reactions at intermediate energies constrain the slope of the symmetry energy. Using this constraint, we show that the radius (radiation radius) of a 1.4 solar mass (M_{\odot}) neutron star is between 11.5 (14.4) and 13.6 (16.3) km.

Key words:

PACS: 25.70.-z, 26.60.+c, 97.60.Jd, 24.10.-i

With central pressures of 10^{36} dynes/cm² and gravitational binding energies of 10^{53} ergs, neutron stars are among the most exotic objects in the universe. Impressive progress has been made on the observable properties of neutron stars, such as masses, radii, spectra, and rotational properties [1,2,3,4,5,6,7,8]. However, a precise neutron star radius measurement still eludes us.

The theoretical understanding of these observable properties demands an understanding of the relevant nuclear physics. For recent reviews, see Refs. [9,10,11,12,13,14,15,16,17]. The global properties of neutron stars: masses, radii, and composition, are determined by the Equation of State (EOS) of neutron-rich nucleonic matter, thus neutron stars are ideal astrophysical laboratories for investigating the

Email address: Bao-An.Li@Tamu-Commerce.edu (Bao-An Li).

EOS. The EOS can be separated into two contributions, the isospin symmetric part (the EOS of nuclear matter, E_{nuc}) and the isospin asymmetric part (the nuclear symmetry energy, E_{sym}). This separation is manifest in the relation $E(\rho, \delta) = E_{\text{nuc}}(\rho) + \delta^2 E_{\text{sym}}(\rho)$, where ρ is the baryon density, $\delta = (\rho_n - \rho_p)/\rho$ is the isospin asymmetry, and ρ_n and ρ_p are the neutron and proton densities. While many neutron star properties depend on both parts of the equation of state, the radius is primarily determined by the slope of the symmetry energy, $E'_{\text{sym}}(\rho)$ [9,10,11,12]. Unfortunately, our knowledge about the density dependence of the nuclear symmetry energy has been rather poor. Predictions of the symmetry energy by nuclear many-body theories vary significantly [18]. Because of its importance for neutron star structure, determining the density dependence of the symmetry energy has been a major goal of the intermediate energy heavy-ion community. Although extracting the symmetry energy is difficult because of the complicated role of isospin in the reaction dynamics, several observable probes of the symmetry energy have been suggested [19,20,21,22] (see also Refs. [23,24,25] for reviews).

Some significant progress has been made recently in determining the density dependence of $E_{\text{sym}}(\rho)$ using: (i) isospin diffusion in heavy-ion reactions at intermediate energies as a probe of the $E_{\text{sym}}(\rho)$ around the saturation density [26,27,28,29,30,31], (ii) flow in heavy-ion collisions at higher energies to constrain the equation of state of nuclear matter [24], and (iii) the sizes of neutron skins in heavy nuclei to constrain $E_{\text{sym}}(\rho)$ at sub-saturation densities [32,33,17,34].

The observational determination of a neutron star radius from the measured spectral fluxes relies on a numerical model of the neutron star atmosphere and uses the composition of the atmosphere, a measurement of the distance, the column density of x-ray absorbing material, and the surface gravitational redshift as inputs. Many of these quantities are difficult to measure, thus the paucity of radius measurements. Current estimates obtained from recent x-ray observations have given a wide range of results.

In this Letter, we combine recently obtained isospin diffusion data, information from flow observables, studies on the neutron skin of ^{208}Pb , and other information to constrain the radius of $1.4 M_{\odot}$ neutron stars.

We use the EOS corresponding to the potential [35,36,37]

$$\begin{aligned}
U(\rho, \delta, \vec{p}, \tau, x) = & A_u(x) \frac{\rho_{\tau'}}{\rho_0} + A_l(x) \frac{\rho_{\tau}}{\rho_0} \\
& + B \left(\frac{\rho}{\rho_0} \right)^{\sigma} (1 - x \delta^2) - 8\tau x \frac{B}{\sigma + 1} \frac{\rho^{\sigma-1}}{\rho_0^{\sigma}} \delta \rho_{\tau'} \\
& + \frac{2C_{\tau, \tau}}{\rho_0} \int d^3 p' \frac{f_{\tau}(\vec{r}, \vec{p}')}{1 + (\vec{p} - \vec{p}')^2 / \Lambda^2} \\
& + \frac{2C_{\tau, \tau'}}{\rho_0} \int d^3 p' \frac{f_{\tau'}(\vec{r}, \vec{p}')}{1 + (\vec{p} - \vec{p}')^2 / \Lambda^2}. \tag{1}
\end{aligned}$$

Here $\tau = 1/2$ ($-1/2$) for neutrons (protons) with $\tau \neq \tau'$, $\sigma = 4/3$, and $f_{\tau}(\vec{r}, \vec{p})$ is the phase space distribution function. The incompressibility K_0 of symmetric nuclear matter at ρ_0 is set to be 211 MeV. Eq. 1 is an extension of the potential from Welke et al. [38,39] from symmetric to asymmetric matter. The parameter x was introduced to mimic various predictions on $E_{\text{sym}}(\rho)$ by using different many-body theories and effective interactions. It is a convenient way to parameterize the uncertainty in the magnitude and density dependence of the symmetry energy while keeping the isospin-symmetric part of the EOS unchanged. The functions $A_u(x)$ and $A_l(x)$ depend on x according to $A_u(x) = -95.98 - x \frac{2B}{\sigma+1}$, and $A_l(x) = -120.57 + x \frac{2B}{\sigma+1}$ such that the same saturation properties of symmetric matter and a value of $E_{\text{sym}}(\rho_0) = 32$ MeV are obtained.

The isoscalar potential estimated from $(U_{\text{neutron}} + U_{\text{proton}})/2$ agrees very well with predictions from variational many-body theory [40]. In addition to being useful at the lower energies discussed here, the underlying EOS has been tested successfully against nuclear collective flow data in relativistic heavy-ion reactions [38,39,24,41] for densities up to five times saturation density. Also, the strength of the momentum-dependent isovector potential at ρ_0 estimated from $(U_{\text{neutron}} - U_{\text{proton}})/2\delta$ agrees very well with the Lane potential extracted from nucleon-nucleus scatterings and (p,n) charge exchange reactions with beam energies up to about 100 MeV [36,37,42,43].

We focus on the properties of spherically-symmetric, non-rotating, non-magnetized neutron stars at zero temperature by solving the Tolman-Oppenheimer-Volkov equation. For the equation of state below about 0.07 fm^{-3} , we use the results from Refs. [44,45]. Also, we assume that the neutron star consists of $npe\mu$ matter, but does not contain any exotic components, such as hyperons, quarks, or Bose condensates.

In Fig. 1 we display some of the basic properties of the EOS and the corresponding neutron stars. Shown in the lower panel is the symmetry energy for $x = 0, -1$ and -2 , respectively. With $x = 0$ the symmetry energy agrees very well with the prediction from Akmal, et. al. (APR) [46] up to about $5\rho_0$. Around ρ_0 , the $x = 0$ EOS can be well approximated by $E_{\text{sym}}^{x=0}(\rho) \approx 32(\rho/\rho_0)^{0.7}$. With $x = -1$, the $E_{\text{sym}}^{x=-1}(\rho) \approx 32(\rho/\rho_0)^{1.1}$ is closer to predictions of typical

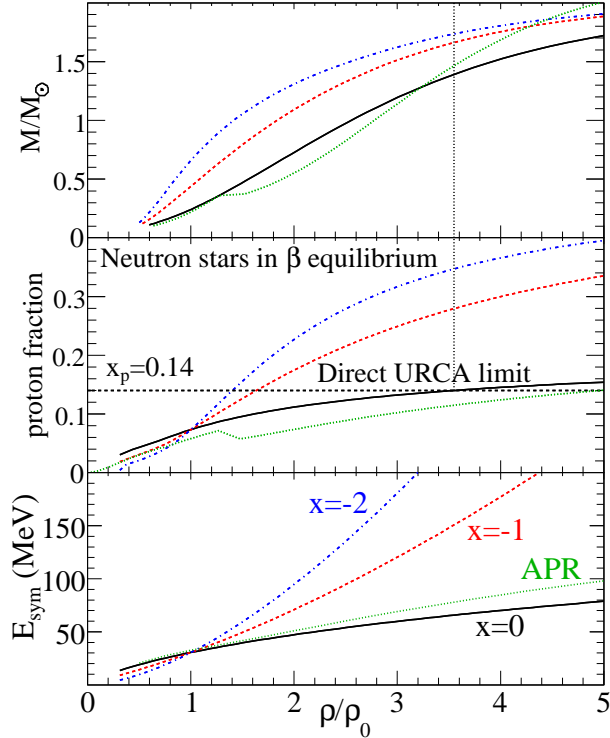


Fig. 1. Neutron star mass as a function of the central density, and the proton fraction for beta-equilibrated matter and symmetry energy as a function of density for the EOS with $x = 0, -1,$ and -2 . The dotted lines give the corresponding results for the APR EOS.

relativistic mean field models [17].

The middle panel shows the proton fraction, x_p , as a function of density, and the top panel gives the mass of a neutron star as a function of the central density. For x_p below 0.14 [47], the direct URCA process does not proceed because energy and momentum conservation cannot be fulfilled. The proton fraction is sensitive to the slope of the symmetry energy [9,10,11,12]. For the $x = -1$ and $x = -2$ EOSs, the condition for direct URCA is fulfilled for nearly all neutron stars above $1 M_\odot$. For the $x = 0$ EOS, the minimum density for direct URCA is indicated by the vertical dotted line, and the corresponding minimum neutron star mass is indicated by the horizontal dotted line. For the $x = 0$ EOS, neutron stars with masses above $1.39 M_\odot$ will have a central density above the threshold for the direct URCA process.

Isospin diffusion in heavy-ion reactions is the re-distribution process of isospin asymmetries carried originally by the colliding partners. The degree and rate of this process depends on the relative pressures of neutrons and protons, namely the slope of the $E_{\text{sym}}(\rho)$. It is harder for neutrons and protons to mix up with a stiffer $E_{\text{sym}}(\rho)$, leading to a smaller/slower isospin diffusion. Moreover, the distribution of the isospin asymmetry versus density during heavy-ion reac-

tions is completely determined by the $E_{\text{sym}}(\rho)$. As an illustration, shown in the insert of Fig. 2 is a snapshot at 20 fm/c of the correlation between the local isospin asymmetry and density in the $^{124}\text{Sn}+^{124}\text{Sn}$ reaction using the two extreme density dependences of the $E_{\text{sym}}(\rho)$. In this work, our calculations of nuclear reactions are performed using the latest isospin and momentum-dependent transport model using in-medium nucleon-nucleon cross sections consistent with the corresponding single particle potential [30]. With the very stiff symmetry energy of $x = -2$, a very neutron-rich dilute cloud surrounds a more symmetric denser region up to $1.6\rho_0$. With the very soft symmetry energy of $x = 1$ (it first rises then starts decreasing with the increasing ρ above about $1.3\rho_0$ [35], mimicking one of the results in Ref. [48]), however, the isospin asymmetries at both very low and very high densities are higher than the average asymmetry of the reaction system. The observed inverse relationship between the $\delta(\rho)$ and $E_{\text{sym}}(\rho)$ is consistent with the well-known isospin fractionation phenomenon first predicted based on the thermodynamics of asymmetric matter [49,50]. Similar to neutron skins in heavy nuclei, neutron-rich clouds are dynamically generated in heavy-ion reactions via the isospin diffusion. This indicates that the same underlying physics is at work [29].

In the following, we examine the strength of the isospin diffusion and the thickness of neutron skin in ^{208}Pb as a function of the slope parameter $L \equiv 3\rho_0(\partial E_{\text{sym}}/\partial\rho)_{\rho_0}$. The degree of isospin diffusion in the reaction of $A+B$ is experimentally measured by using [51]

$$R_i \equiv \frac{2O_I^{A+B} - O_I^{A+A} - O_I^{B+B}}{O_I^{A+A} - O_I^{B+B}}, \quad (2)$$

where O_I is any isospin-sensitive observable. The frequently used ones include the neutron/proton ratio of pre-equilibrium nucleons, ratios of light mirror nuclei and the isospin asymmetry of projectile-like fragments. They all give essentially the same result [27,52]. By construction, the value of R_i is 1 (-1) for the symmetric $A + A$ ($B + B$) reaction. If a complete isospin equilibrium is reached in the asymmetric reaction $A + B$ as a result of isospin diffusion the value of R_i is about zero. The R_i also has the advantage of reducing significantly its sensitivity to the symmetric part of the EOS. Shown in Fig. 2 are the strength of isospin diffusion $1 - R_i$ calculated using the transport model[30] and the size of neutron skin dR_{np} in ^{208}Pb calculated using the Skyrme Hartree-Fock with interaction parameters adjusted such that the same EOS is obtained [29]. The strength of isospin diffusion $1 - R_i$ is seen to decrease, while dR_{np} increases with the increasing L as one expects. The NSCL/MSU data $1 - R_i = 0.525 \pm 0.05$ implies that the $L(X)$ parameter is constrained between 62.1 MeV ($x=0$) and 107.4 MeV ($x=-1$). This is consistent with the measurement $dR_{np} = 0.2 \pm 0.04$ fm [53] and also with several recent calculations [17,32,33,34]. However, presently available measurements of the neutron skin thickness using hadronic probes have large systematic

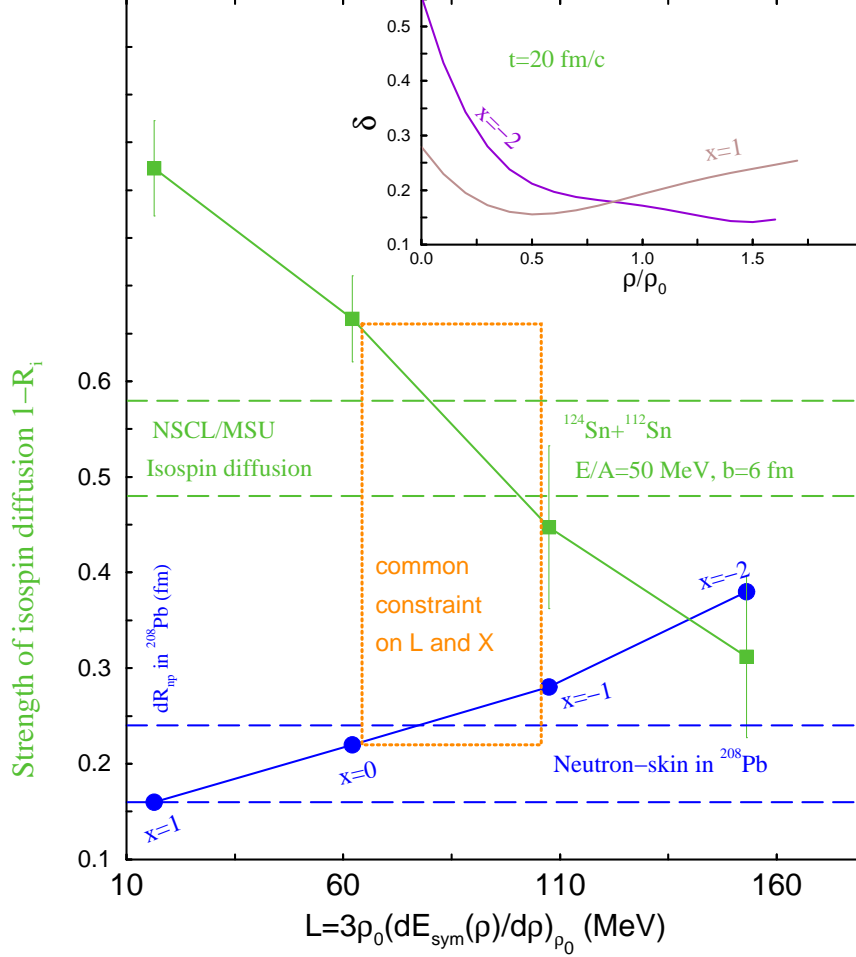


Fig. 2. The strength of isospin diffusion in the $^{124}\text{Sn}+^{112}\text{Sn}$ reaction and the size of neutron skin in ^{208}Pb as a function of the slope of the symmetry energy, respectively. The insert is the correlation of the isospin asymmetry and density at the instant of 20 fm/c in the reaction considered.

uncertainties associated with the strong interaction.

The corresponding mass vs. radius curves for these EOSs, as well as for APR (using the AV18+ δv +UIX* interaction) are given in Fig. 3. In addition the constraints of causality, the mass-radius relation from estimates of the crustal fraction of the moment of inertia ($\Delta I/I = 0.014$) in the Vela pulsar [54], and the mass-radius relation from the redshift measurement from Ref. [56] are given. Any equation of state should be to the right of the causality line and the $\Delta I/I$ line and should cross the $z = 0.35$ line. The horizontal bar indicates the inferred limits on the radius and the radiation radius (the value of the radius which is observed by an observer at infinity) defined as $R_\infty = R/\sqrt{1 - 2GM/Rc^2}$ for a $1.4 M_\odot$ neutron star.

Since all three calculations with $x = 0, -1$ and $x = -2$ have the same compressibility ($K_0 = 211$ MeV) but rather different radii, it is clear that the

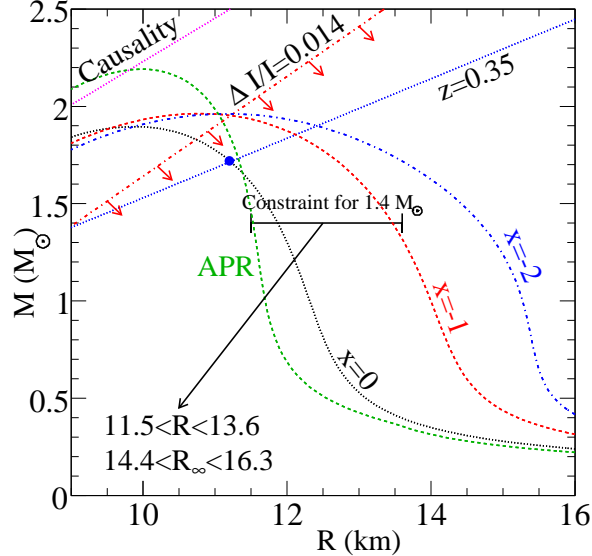


Fig. 3. The mass-radius curves for $x = 0, -1$, and -2 and the APR EOS. The limit from causality, the Vela pulsar, and the redshift of EXO0748 are all indicated. The inferred radius of a $1.4 M_{\odot}$ neutron star and the inferred value of R_{∞} are given.

radius is indeed rather sensitive to the symmetry energy while the maximum mass is only slightly modified [9,10,11,12,55]. The APR EOS has a compressibility of $K_0 = 269$ MeV but almost the same symmetry energy as with $x = 0$. We note that the APR EOS leads to a 16% higher maximum mass ($1.9M_{\odot}$ to $2.2M_{\odot}$) but only a 5% decrease in radius (12.0 km to 11.5 km) as compared to the results with $x = 0$.

Since only EOSs with symmetry energies between $x = 0$ and $x = -1$ are consistent with the isospin diffusion data and measurements of the skin thickness of lead, we take them as representative of the possible variation in neutron star structure that is consistent with terrestrial data. The APR and the $x = 0$ EOS have nearly identical symmetry energies and slightly different radii. Neutron star radii are strong functions of the symmetry energy but also contain contributions from the isospin-symmetric part of the EOS, especially at higher densities. Even though the compressibility of the APR EOS is larger than that of the $x = 0$ EOS, the pressure is typically lower in the APR EOS at densities just above saturation, giving the APR EOS a smaller radius by about 5%. Thus we take this 5% difference as representative of the remaining uncertainty in the symmetric part of the EOS and extend the minimum radius to 11.5 km. Neutron stars with radii larger than 13.6 km are difficult to make without a larger symmetry energy or compressibility [17]. We conclude that only radii between 11.5 and 13.6 km (or radiation radii between 14.4 and 16.3 km) are consistent with the $x = 0$ and $x = -1$ EOSs, and thus consistent with the laboratory data. It is interesting to note that a radius of $R=12.66$ km was recently predicted for canonical neutron stars using a new effective interac-

tion calibrated by reproducing several collective modes of ^{90}Zr and ^{208}Pb [34]. This radius falls right in the range of our constraints. Our constraints on the radius are also consistent with the range of radii from the extensive analysis in Ref. [17] with only a few exceptions. The field-theoretical models from this reference which are outside our suggested range either have a relatively large symmetry energy at saturation density (≥ 36 MeV), or have very soft symmetry energies created by extremely strong non-linear couplings which are atypical of most relativistic mean field models.

Our results suggest that the direct URCA processes is likely for stars with masses larger than $1.39 M_{\odot}$, which is the limit obtained from the $x = 0$ EOS in Fig. 1. This constraint nearly matches the constraint for the direct URCA process of $1.30 M_{\odot}$ obtained in Ref. [34]. This is markedly different, however, from the result from APR, which gives a large threshold for the direct URCA process (even though the symmetry energy is very similar to our $x = 0$ EOS).

Does this constraint agree with present neutron star radius observations? The answer to this question is “yes”. Assuming a mass of $1.4 M_{\odot}$, the inferred radiation radius, R_{∞} , (in km) is 13.5 ± 2.1 [3,4] or 13.6 ± 0.3 [5] for the neutron star in ω Cen, 12.8 ± 0.4 in M13 [6], $14.5^{+1.6}_{-1.4}$ for X7 in 47 Tuc [7] and $14.5^{+6.9}_{-3.8}$ in M28 [8], respectively. Except the neutron star in M13 that has a slightly smaller radius, all others fall into our constraints of $14.4 \text{ km} < R_{\infty} < 16.3 \text{ km}$ within the observational error bars that are often larger than the range we gave.

While the Vela $\Delta I/I$ upper limit does not provide any new information, the fact that the $z = 0.35$ line does not cross our range of radii implies a mass larger than $1.4 M_{\odot}$ for EXO-0748 (the minimum mass would be about $1.7 M_{\odot}$ corresponding to the dot in Fig. 3). This is larger than the canonical $1.4 M_{\odot}$ neutron star mass, but is not unreasonable since this object is accreting [56]¹.

While estimates of radii based on astrophysical observations are still very challenging, it is useful to compare our results with recent Chandra/XMM-Newton observations. Together with more refined observations, future heavy-ion experiments (some recent progress in Ref. [58]) with advanced radioactive beam facilities [59] and measurements of parity violating electron-nucleus scattering [60] will allow us to pin down more precisely the EOS of neutron rich matter. This would allow tighter constraints on neutron star radii. On the other hand, a neutron star radius measurement outside of our prediction may indicate non-standard physics.

¹ In fact, while revising this work, a measurement of the mass $2.10 \pm 0.28 M_{\odot}$ and radius $13.8 \pm 1.8 \text{ km}$ for this object was reported in Ref. [57], confirming that this object is likely more massive than $1.4 M_{\odot}$.

We would like to thank Lie-Wen Chen and Sanjay Reddy for helpful discussions and the anonymous referees for their comments. The work of B.A. Li was supported in part by the NSF under Grant No. PHY-0354572, PHY0456890 and the NASA-Arkansas Space Grants Consortium Award ASU15154. The work of A.W. Steiner was supported by the DOE under grant no. DOE/W-7405-ENG-36.

References

- [1] S.E. Thorsett and D. Chakrabarty, *Astrophys J.* 512 (1999) 288.
- [2] P. Haensel, *A&A* 380 (2001) 186.
- [3] R.E. Rutledge et al., *Astrophys J.* 580, (2002) 413.
- [4] R.E. Rutledge et al., *Astrophys J.* 577 (2002) 346.
- [5] B. Gendre, D. Barret and N. A. Webb, *Astron. Astrophys.* 400 (2003) 521.
- [6] B. Gendre, D. Barret and N. Webb, *Astron. Astrophys.* 403 (2003) L11.
- [7] G.B. Rybicki et al., astro-ph/0506563.
- [8] W. Becker et al., *Astrophys. J.* 594 (2003) 798.
- [9] J.M. Lattimer and M. Prakash, *Phys. Rep.* 333 (2000) 121.
- [10] J.M. Lattimer and M. Prakash, *Astr. Phys. Jour.* 550 (2001) 426.
- [11] J.M. Lattimer and M. Prakash, *Science Vol.* 304 (2004) 536.
- [12] M. Prakash, J.M. Lattimer, R.F. Sawyer and R.R. Volkas, *Ann. Rev. Nucl. Part. Sci.* 51 (2001) 295.
- [13] D.G. Yakovlev and C.J. Pethick, *Ann. Rev. Astron. Astrophys.* 42 (2004) 169.
- [14] P. Haensel, in: *Final Stages of Stellar Evolution*, eds. J.-M. Hameury and C. Motch, EAS Publications Series (EDP Sciences, 2003).
- [15] H. Heiselberg and V.R. Pandharipande, *Ann. Rev. Nucl. Part. Sci.* 50 (2000) 481.
- [16] H. Heiselberg and M. Hjorth-Jensen, *Phys. Rep.* 328 (2000) 237.
- [17] A.W. Steiner, M. Prakash, J.M. Lattimer and P.J. Ellis, *Phys. Rep.* 411 (2005) 325.
- [18] A.E.L. Dieperink *et al.*, *Phys. Rev. C* **68**, 064307 (2003).
- [19] B.A. Li, C.M. Ko and Z. Ren, *Phys. Rev. Lett.* 78 (1997) 1644.
- [20] B.A. Li, *Phys. Rev. Lett.* 85 (2000) 4221.

- [21] B.A. Li, Phys. Rev. Lett. 88 (2002) 192701.
- [22] B.A. Li, C.M. Ko and W. Bauer, Int. J. of Mod. Phys. E7 (1998) 147.
- [23] Isospin Physics in Heavy-Ion Collisions at Intermediate Energies, eds. B.A. Li and W. Udo Schröder (Nova Science Publishers, Inc. New York, 2001).
- [24] P. Danielewicz, R. Lacey and W.G. Lynch, Science 298 (2002) 1592.
- [25] V. Baran, M. Colonna, V. Greco and M. Di Toro, Phys. Rep. 410 (2005) 335.
- [26] L. Shi and P. Danielewicz, Phys. Rev. C68 (2003) 064604.
- [27] M.B. Tsang et al., Phys. Rev. Lett. 92 (2004) 062701.
- [28] L.W. Chen, C.M. Ko and B.A. Li, Phys. Rev. Lett. 94 (2005) 032701.
- [29] A.W. Steiner and B.A. Li, Phys. Rev. C72 (2005) 041601(R).
- [30] B.A. Li and L.W. Chen, Phys. Rev. C72 (2005) 064611.
- [31] L.W. Chen, C.M. Ko and B.A. Li, Phys. Rev. C72 (2005) 064309.
- [32] C.J. Horowitz and J. Piekarewicz, Phys. Rev. Lett. 86 (2001) 5647.
- [33] C.J. Horowitz and J. Piekarewicz, Phys. Rev. C66 (2002) 055803.
- [34] B.G. Todd-Rutel and J. Piekarewicz, Phys. Rev. Lett. 95 (2005) 122501.
- [35] C.B. Das, S. Das Gupta, C. Gale and B.A. Li, Phys. Rev. C67 (2003) 034611.
- [36] B.A. Li, C.B. Das, S. Das Gupta, C. Gale, Phys. Rev. C69, (2005) 011603(R).
- [37] B.A. Li, C.B. Das, S. Das Gupta, C. Gale, Nucl. Phys. A735 (2004) 563.
- [38] G.M. Welke, M. Prakash, T.T.S. Kuo, et al., Phys. Rev. C38 (1988) 2101.
- [39] C. Gale, G.M. Welke, M. Prakash, et al., Phys. Rev. C41 (1990) 1545.
- [40] R.B. Wiringa, Phys. Rev. C38 (1988) 2967.
- [41] J. Zhang, S. Das Gupta and C. Gale, Phys. Rev. C50 (1994) 1617.
- [42] G.W. Hoffmann and W.R. Coker, Phys. Rev. Lett. 29 (1972) 227.
- [43] P.E. Hodgson, The Nucleon Optical Model (World Scientific, Singapore, 1994) p. 613.
- [44] J.W. Negele and D. Vautherin, Nucl. Phys A207 (1974) 298.
- [45] G. Baym, C.J. Pethick, and P. Sutherland, Astrophys. J 170 (1971) 299.
- [46] A. Akmal, V.R. Pandharipande and D.G. Ravenhall, Phys. Rev. C58 (1998) 1804.
- [47] J.M. Lattimer, C.J. Pethick, M. Prakash and P. Haensel, Phys. Rev. Lett. 66 (1991) 2701.

- [48] R.B. Wiringa, V. Fiks and A. Fabrocini, Phys. Rev. C38 (1988) 1010.
- [49] H. Müller and B.D. Serot, Phys. Rev. C52 (1995) 2072.
- [50] B.A. Li and C.M. Ko, Nucl. Phys. A618 (1997) 498.
- [51] F. Rami et al., Phys. Rev. Lett. 84 (2000) 1120.
- [52] W.G. Lynch, private communication.
- [53] V.E. Starodubsky and N.M. Hintz, Phys. Rev. C49 (1994) 2118
- [54] B. Link, R. I. Epstein and J.M. Lattimer, Phys. Rev. Lett. 83 (1999) 3362.
- [55] M. Prakash, T.L. Ainsworth and J.M. Lattimer, Phys. Rev. Lett. 61 (1988) 2518.
- [56] J. Cottam, F. Paerels, and M. Mendez, Nature 420 (2002) 51.
- [57] F. Ozel, Nature 441 (2006) 1115.
- [58] M. A. Famiano, et al., Phys. Rev. Lett. 97, 052701 (2006).
- [59] RIA Theory Bluebook, www.ornl.gov/ria/RIATG
- [60] C.J. Horowitz, S.J. Pollock, P.A. Souder and R. Michaels, Phys. Rev. C63 (2001) 025501.